Seasonal dynamics in picocyanobacterial abundance and clade composition at coastal and offshore stations in the Baltic Sea

Javier Alegria Zufia
Linnaeus University
Catherine Legrand
Halmstad University
Hanna Farnelid (hanna.farnelid@lnu.se)
Linnaeus University

Article

Keywords:

Posted Date: April 15th, 2022

DOI: https://doi.org/10.21203/rs.3.rs-1521980/v1

Abstract

Picocyanobacteria (< 2 µm in diameter) are significant contributors to total phytoplankton biomass. Due to the high diversity within this group, their seasonal dynamics and relationship with environmental parameters, especially in brackish waters, are largely unknown. In this study, the abundance and community composition of phycoerythrin rich (PE-rich) and phycocyanin rich (PC-rich) picocyanobacteria were monitored at a coastal (K-station) and at an offshore station (LMO; ~10 km from land) in the Baltic Sea over three years (2018–2020). Cell abundances of picocyanobacteria correlated positively to temperature and negatively to nitrate (NO_3) concentration. While PE-rich abundance correlated to the presence of nitrogen fixers, PC-rich abundance was linked to stratification/shallow waters. The picocyanobacterial targeted amplicon sequencing revealed an unprecedented diversity of 2169 picocyanobacterial amplicons sequence variants (ASVs). A unique assemblage of distinct picocyanobacterial clades across seasons was identified. Clade A/B dominated the picocyanobacterial community, except during summer when low NO_3 and high phosphate (PO_4) concentrations and warm temperatures promoted S5.2 dominance. This study, providing multiyear data, bridges the gap between *Synechococcus/Cyanobium/Synechocystis* phylogenetic classification and ecology. The difference in the response of the two functional groups and clades underscore the need for further high-resolution studies to understand their role in the ecosystem.

Introduction

Unicellular picocyanobacteria (< 2 µm in diameter) belonging to *Synechococcus/ Cyanobium/Synechocystis* genus (SYN) are highly adaptable and widespread in aquatic ecosystems[1]. The genus is polyphyletic [2,3] and is characterized by a high diversity in terms of pigment content [4], taxonomy [5] and physiology [6]. SYN populations are a major contributor to carbon flux in oligotrophic oceans [7,8] as well as coastal, estuarine and freshwaters [9–11]. However, there are relatively few studies that focus on SYN dynamics and community composition in freshwater [12–14] and estuarine waters [15–17] despite showcasing higher diversity than their marine counterparts [18]. Under climate change scenarios, the abundance of SYN cells is expected to increase [1,19] while the rest of the phytoplankton community biomass is expected to decrease[20,21]. Understanding the distribution and dynamics of SYN ecotypes is therefore of high interest for evaluating ecosystem consequences.

Distribution and seasonal occurrence of marine phylogenetic clades have been linked to environmental factors, increasing our understanding on marine SYN dynamics and distribution [22–24]. SYN populations are composed of unicellular phycoerythrin (PE)-rich cells (adapted to blue and green light) and phycocyanin (PC)-rich cells (adapted to red light). It has been observed that PE-rich is more prevalent in low turbidity waters (generally open waters), while PC-rich is better adapted to turbid waters (generally coastal waters) [25–29]. Other factors, such as water column stability and stratification can also have a significant effect on the PE:PC ratios [30,31]. Peak SYN cell abundance is normally recorded during periods of warm temperatures and low nutrient concentration [8,32]. SYN cells may use ammonium (NH_4) from

nitrogen (N_2)-fixers or benthic regeneration as main source of nitrogen [33–35]. Other nutrients such as phosphate (PO_4) have also been observed to have an effect on picocyanobacterial dynamics and distribution [36].

Pigment related genes *cpcBA*, *mpeBA*, and *mpeW* have been used to describe its diversity [37]. Studies based on 16S rDNA, 16S-23S internally transcribed spacer (ITS), petB, psbB, rpoC1, narB genes as well as full genome analysis have provided more detailed phylogeny despite not being directly related to the pigment content or other morphological characteristics [38–45]. Phylogenetically, SYN populations can be divided into three subclusters: S5.1, composed strictly of marine strains, S5.2, containing both marine and brackish adapted strains and S5.3 containing mainly oceanic strains from surface waters [22,46–49]. These subclusters can be further divided into 20 well defined clades, which are closely related to the physio-ecological characteristics of SYN [50,51]. In addition, there are a number of brackish and freshwater clades that do not subscribe to any of the subclusters [12,18].

The Baltic Sea is characterized by a salinity gradient from 2.9 PSU in the Bothnian Bay to 22 PSU in the Kattegat. In the Baltic Proper, picocyanobacterial blooms take place during the summer at temperatures up to 20–24°C and nitrogen limited conditions [52–54]. Peak abundances during this period reach up to 10^5 cells mL^{-1} [53,55] corresponding to 21% contribution to the total phytoplankton community in terms of Chl *a* [56] and 56% in terms of carbon biomass [53]. The diversity of the picocyanobacterial community in the Baltic Sea has been characterized by amplification and sequencing of the V4-V5 16S rDNA gene hypervariable region (e.g. [6,15,17,57]). SYN sequences can dominate the sequence libraries [6,17]. During summer, the SYN populations are dominated by brackish strains from the S5.2 in the North, and there is a transition towards a community dominated by S5.1 at 13–16 PSU in the South [17]. Amplification and sequencing of the pigment genes for PE (*cpeBA*) and PC (*cpcBA*) showed that the Baltic Sea is equally populated by PE-rich and PC-rich in the upper 30 m of the water column [30]. In the summer, the SYN population is dominatied by an ecotype with a novel pigment gene which was recently genomically characterized in a metagenome-assembled genome (MAG) reconstructed from the Baltic Proper (BACL30) [16]. The discovery of this unique brackish strain is linked to the existence of global brackish microbiome [58,59]. The current data suggests that the high physiological diversity of the picocyanobacterial community shows adaptation for different temperatures and nutrient regimes [6] but few annual studies have been conducted which limits the understanding of seasonal dynamics.

Recently, Huber et al., [60] showed that the hypervariable region V5-V7 of the 16S rDNA gene provided high resolution of picocyanobacterial diversity in both marine and freshwater environments. An accurate phylogenetic clade classification over multiple years in the dynamic Baltic Sea can help to disentangle the drivers of SYN and fill knowledge gaps of brackish and freshwater strains. Here we monitored the abundance of SYN cells with flow cytometry and studied its clade community composition at high-resolution during three consecutive years at a coastal and an offshore station. This study provides with

novel information on the relationship between SYN pigment ecotypes and phylogenetic clades with environmental parameters in a brackish environment.

Results

Environmental conditions

Water was sampled biweekly at the Linnaeus Microbial Observatory (LMO, 56°55'51.24"N, 17°3'38.52"E, 2 m sampling depth), an offshore station located 10 Km off the east coast of Öland (Sweden) and weekly at the K-station, a coastal station located in the city of Kalmar, Sweden (56°39'25.4"N 16°21'36.6"E, 1 m sampling depth) during 2018–2020. Seawater temperature ranged from 0 to 5°C during winter at both stations and increased during spring (~ 3–15°C) and summer (~ 15–20°C) (Fig. 1A). In 2018, there was an earlier increase of temperature during summer compared 2019 and 2020 (average 3°C higher in the beginning of June) and the maximum temperatures during the study period were recorded; 24°C and 22°C at the K-station and LMO respectively. At LMO, the increase of temperature during summer resulted in water depth stratification (mixed layer approx. depth: 20 m) that lasted until early to mid-autumn (N^2: $0.2–0.66 \times 10^{-3}$ s^{-2}) (Supplementary Fig. S2A and B). In 2018, early signs of stratification were observed during spring due to the exceptionally high temperatures. Salinity ranged between 6.5 and 8 PSU (Fig. 1B). At the K-station, salinity increased during the spring to summer period while no clear seasonality was observed at the LMO. Inorganic nitrogen (NO_3) concentrations ranged between 5 and < 0.06 (detection limit) µM, with the highest concentrations observed at the K-station during winter, which sharply declined upon temperature increase during spring down to < 0.06 (Fig. 1C). Phosphate concentrations (PO_4) decreased during spring (from 1 to 0.2 µM) and remained low throughout the summer with occasional peaks up to 1 µM at the K-station (Fig. 1D). At the K-station, silicate (SiO_2) showed a strong seasonality ranging from 4 to 25 µM with peaks in summer and early autumn (Fig. 1E). Silicate did not show a clear seasonality at LMO: concentrations ranged between 10 and 20 µM during 2018, sharply declined during spring in 2019 and remained stable around 5 µM.

Phytoplankton dynamics

Chl *a* was generally higher at the K-station (1–7 µg $L^{-1)}$ compared to LMO (1-4.5 µg L^{-1}) (Fig. 2A). At the K-station phytoplankton carbon biomass increased from 0.35 mg C mL^{-1} in the autumn to winter period up to 50 mg C mL^{-1} in the spring and 147.68 mg C mL^{-1} in the summer (Fig. 2A). The phytoplankton community was dominated by diatoms during autumn, winter and first half of the spring. During the second half of the spring the community transitioned to ciliates and dinoflagellates dominance (Fig. 2C). N_2-fixers (filamentous cyanobacteria) were only observed during the summer 2018, reaching 111.24 mg C mL^{-1} in July.

At the LMO the maximum carbon biomass increased from 5.85 mg C mL^{-1} in the autumn and winter up to 597.39 mg C mL^{-1} in the spring and 167.69 mg C mL^{-1} in the summer (Fig. 2B). During the autumn, winter and spring, the community is dominated by ciliates and dinoflagellates (Fig. 2D), and occasionally

by diatoms. During the summer the phytoplankton community was dominated by N_2-fixers, reaching 111.24 mg C mL^{-1} total carbon biomass.

Picocyanobacterial dynamics

PE-rich showed low concentration in the winter (LMO: 2.7×10^2 cells mL^{-1}, K-station: 8.2×10^2 cells mL^{-1}) and showed peak abundances in the period from spring to summer (3.8×10^5 cells mL^{-1}) and summer to autumn (2.6×10^5 cells mL^{-1}) in the K-station and LMO respectively (Fig. 2E). PC-rich increased from low concentrations in the winter (K-station: 72 cells mL^{-1}, LMO: 8 cells mL^{-1}) to peak concentrations during spring and summer (K-station: 2.1×10^5 cells mL^{-1}, LMO: 4.8×10^3 cells mL^{-1}) (Fig. 2F).

To analyze the effect of each independent variable on PE-rich and PC-rich abundance, we used the PLS method to establish a regression equation. The number of components utilized for each equation was 2 and 6 for PE-rich and PC-rich respectively. Only the independent variables with VIP > 1 were considered relevant for the final equation (Table 1). The model for PE-rich explained 38% of the cell abundance seasonal changes with 52% of the independent variables variation. The regression equation between PE-rich cell abundance and the independent variables was as follows (1):

Table 1
VIP values of each variable.

	NO_3	PO_4	SiO_2	Temperature	Salinity	Biomass	N_2 fixers	Strat. index
PE-rich	1.18	0.58	0.74	1.71	0.27	0.80	1.28	0.59
PC-rich	1.54	0.51	0.27	1.47	0.81	0.15	0.44	1.49

$$(1)\ y = -0.05 \cdot NO_3(\mu M) + 0.25 \cdot T\ (C°) + 0.16 \cdot N_2\text{-}Fixers\ (mgC \cdot mL^{-1})$$

The model for PC-rich explained 40% of the cell abundance seasonal changes with 46% of the independent variables variation. The regression equation between PC-rich cell abundance and the independent variables was (2):

$$(2)\ y = -0.23 \cdot NO_3(\mu M) + 0.21 \cdot T\ (C°) + 0.21 \cdot S\ (PSU) + 0.28 \cdot N^2(10^{-3}\ s^{-2})$$

Picocyanobacteria community composition

In total, there were 2169 ASVs identified as SYN in the amplicon libraries. At the LMO the number of ASVs remained more stable throughout the seasons. The ASVs were affiliated with 9 different subgroups and clades: Bornholm, subalpine II, S5.1, S5.2, Ib and the newly defined A/B, KS 1, KS 2, KS 3 and KS 4. Clade A/B was defined as a combination between clade A and clade B, since the V5-V7 region of the 16S rRNA

gene targeted in this study did not allow for a clear separation between these two clades. 39 ASVs represented > 1% of picocyanobacterial sequences in one sample, of which only one ASV belonged to the marine S5.1 clade (Supplementary Fig. S3), eight belonged to the S5.2 clade, 15 belonged to clade A/B and the rest were divided among freshwater clades (H, Subalpine I, Bornholm, Ib, KS1, KS2, KS3, KS4, KS5 and KS6). ASVs within clade A/B dominated at both stations during autumn (maximum contribution at the K-station 2018-11-10: 92% and LMO 2020-11-26: 92%), winter (maximum contribution at the K-station 2020-11-10: 90% and LMO 2019-02-19: 96%) and spring (maximum contribution at the K-station 2019-05-14: 98% and LMO 2020-05-26: 98%). During summer, the K-station libraries were dominated by S5.2 (maximum contribution 2019-08-13: 91%), followed by an increase in KS3 at the end of the summer to beginning of autumn (maximum contribution 2019-10-08: 68%). At the LMO the period of late summer to early autumn was occasionally dominated by S5.2 (maximum contribution 2018-09-11: 68%). The picocyanobacterial community was more diverse in the coastal K-station compared to the offshore LMO (K-station registered 1026 ASVs and LMO registered 195 ASVs). The phylogenetic classification (which only includes ASVs that represented > 1% of the sequences in at least one sampling point) showed that some sequences that belong to the clades KS2 (ASV00070), KS5 (ASV07850) KS6 (ASV00066) and S5.2 (ASV07854 and ASV07849) were only present in the coastal K-station. The number of ASVs was consistently higher at the K-station, with the highest numbers of ASVs present during autumn to early spring (Fig. 3).

Correlations between environmental and biological variables with picocyanobacterial composition

The Procrustes analysis and squared m12 of the CAs revealed a significant association between the distribution of the phylogenetic clades and ASVs (P-value < 0.001, Supplementary Fig. S4). The stepwise CCA showed a significant relationship between clade composition and eight environmental and biological variables: NO_3 (µM), SiO_2 (µM), PO_4 (µM), temperature (°C), salinity (PSU), N_2-fixers biomass (mg C mL^{-1}), PE-rich (cells mL^{-1}) and PC-rich (cells mL^{-1}) (Table 2). The first two axis explained 49% of the taxonomic composition (Fig. 4). The first axis indicated a clear separation of summer samples. Summer samples were associated with high abundance of PE-rich and PC-rich, increase of temperature and high PO_4. Autumn, winter and spring sites from the model clustered together and were associated with high NO_3. PC-rich abundance and temperature were the most important variables as indicated by the length of the variable arrows (Fig. 4).

Table 2
P-values included in the CCA model after stepwise analysis. Significant variables after the Holm correction are indicated in bold.

	R2.adj	Df	AIC	F	P-value
PC-rich	**0.22**	**1**	**-10.93**	**39.90**	**0.001**
Temperature	**0.28**	**1**	**-20.21**	**11.50**	**0.001**
PO_4	**0.33**	**1**	**-29.96**	**11.91**	**0.001**
PE-rich	**0.37**	**1**	**-36.20**	**8.18**	**0.001**
N_2-fixers	**0.38**	**1**	**-38.86**	**4.53**	**0.003**
SiO_2	**0.40**	**1**	**-41.95**	**4.91**	**0.002**
NO_3	**0.41**	**1**	**-44.12**	**3.99**	**0.004**
PPE	0.43	1	-45.15	2.86	0.018
N^2	0.43	1	-48.53	2.96	0.017
Salinity	**0.45**	**1**	**-29.959**	**3.94**	**0.007**

Discussion

This study shows that temperature was one of the main parameters driving picocyanobacterial abundance. The correlation between temperature and increase in picocyanobacterial abundance is well known in both marine [8,9] and freshwater systems [61,62]. Picocyanobacterial abundance started increasing at > 10°C, in line with other temperate ecosystems (e.g. [63]) and previous records in the Baltic Sea [9]. Peak abundances at the coastal K-station and offshore LMO during 2019 and 2020 were in the same range, with the exception of the summer of 2018, when K-station peak abundances reached 4.7×10^5 cells mL^{-1}. These numbers are comparable to other observations in the Baltic Sea Proper during summer (10^5 cells mL^{-1}) [55,64], and confirm previous observations that picocyanobacterial abundances are as high in coastal and offshore locations [53]. It is also important to note that the picocyanobacterial abundances at < 10°C reported in this study were notably higher than previous reports in the Gulf of Finland and in other temperate ecosystems [8,9]. The ecological niche for SYN has recently been defined as > 5°C [19]. However, in this study abundances of > 10^4 cells mL^{-1} were recorded during winter time at both K-station (0-5.7°C) and LMO (2.7–5.8°C), suggesting that the strains present in the Baltic Sea are well adapted to low temperatures, in line with previous observations by Paulsen et al., [65].

According to the PLS models independent variables only explained 38 and 40% of the total variation of PE-rich and PC-rich respectively. This indicates other important controllers such as light quality [4], grazing

by ciliates and flagellates [66] or viral lysis [67] may be important drivers of picocyanobacterial abundances should be included in future models.

SYN was divided into PE-rich and PC-rich depending of the pigment content. PE-rich and PC-rich coexisted at similar abundances during the summer, confirming previous observations based on cpcBA and cpeBA libraries [30]. PE-rich is better adapted to blue light which can penetrate deeper in the mixing layer, while PC-rich is adapted to red light, which is dissipated in the surface [4]. As a result, PE-rich was equally prevalent in both the K-station and the LMO. On the other hand, PC-rich abundance variation was strongly linked to the stratification index (N^2) and was more prevalent in the coastal K-station compared to the offshore LMO, in line with observations in other estuaries and freshwater lakes [31,68]. These results suggest a horizontal gradient on the Baltic Sea, where PC-rich is more prevalent in coastal shallow areas while in offshore areas abundances are lower and tightly joined to stratification seasonality. In future, an increase in the stratification periods as a result of global warming could reinforce PC-rich dominance on the picocyanobacterial community. PC-rich has been observed to have a negative effect on co-occurring filter-feeders, the ability to avoid predation and viral lysis, which can affect the energy flow to upper trophic layers [69–71]. Thus, understanding the physiology and ecology of PC-rich, a generally understudied group of SYN, is of high importance for the understanding of current and future climate scenarios.

Nutrient availability, particularly nitrogen species, was correlated to picocyanobacterial dynamics according to the PLS models. For example, both PE-rich and PC-rich showed moderate negative correlation with NO_3 abundance. Picocyanobacteria (both PE-rich and PC-rich) showed a negative correlation with NO_3 concentration. Several studies have documented the preference of picocyanobacteria for NH_4 over NO_3 at high temperature conditions (> 15°C) [53,72]. Thus, newly fixed nitrogen in the form of NH_4 from N_2-fixers may be a main driver supporting picocyanobacterial growth during summer [33–35], in line with the positive correlation between N_2-fixers and PE-rich. However, PE-rich peak abundances at the K-station and LMO were in the same range, although N_2-fixers were only observed at the K-station during 2018. This suggests that PE-rich can benefit from newly fixed nitrogen, but it is not a requirement to achieve peak abundances and thus other nitrogen pools should also be considered. In fact, the main nitrogen source for picocyanobacteria during the summer could be originated from benthic regeneration, which in coastal and shallow water areas (< 50 m depth) can represent up to 97% of the nutrient requirements [35,73]. In addition, peak abundances at the LMO are sustained during the first half of the autumn at < 10°C, which indicates that picocyanobacteria can uptake NO_3 at low concentrations efficiently.

The community composition was studied using 16S rRNA gene sequences amplified using specific primers that target almost exclusively picocyanobacteria [60]. The results corroborate that the V5-V7 region of the 16S rRNA gene showcases higher variability in picocyanobacteria than the V3-V4 region, revealing an unprecendented high strain diversity in the Baltic Sea with a particularly high number of ASVs at the coastal K-station. Most of the previously defined clades and clusters were described [60], but some clusters

were altered. For example, clades A and B clustered together (clade A/B) contrasting with phylogeny based on other regions of the 16S rRNA gene [12,74]. All ASVs in clade A/B displayed similar seasonal variation in relative abundance, suggesting a similar ecophysiology whithin the clade. The increase in contribution of S5.2 took place in June-July, when temperature was > 18°C and NO_3 concentration was low. This result suggests that S5.2 affiliated picocyanobacterial strains are adapted to high temperatures and may use NH_4 as a primary nitrogen source [35,53,72]. On the other hand, clade A/B dominated during the colder months, indicating that picocyanobacteria strains in this clade are well adapted to low temperatures and high NO_3 concentration.

This study indicates a coastal to offshore differentiation in picocyanobacterial community composition. The coastal K-station presented higher ASV diversity than the offshore LMO. Moreover, the clades KS2, KS5 and KS6 were only present in the coastal K-station, which suggest that some clades are only present in the coastal region. These results contradicts previous observations in the Baltic proper where no differences in community composition were observed in coastal offshore gradients [6]. One explanation is that the higher resolution achieved with the primers in this study have revealed differences that could not be detected with less specific primers. Community composition seasonal dynamics in the coastal and offshore stations also showed major differences. At the K-station picocyanobacterial peak abundances took place when S5.2 was dominating the community while at the LMO peak abundances took place under clade A/B dominance. The different dynamics at the coastal compared to the offshore station could be driven by low PO_4 levels as S5.2 was positively linked to PO_4 concentration. At the LMO, PO_4 was low during summer (0-0.32 µM) while it remained high at the K-station (0-1.5 µM), explaining the lower contribution of S5.2 in the LMO. The potential PO_4 limitation could also explain why at the LMO S5.2 has lower contributions during summer to the community composition compared to the K-station. However, to fully understand picocyanobacterial dynamics, other parameters such as light hours [75], NH_4 recycling rates [35] or nutrient competition with specific phytoplankton groups [72] should also be considered.

The most abundant ASV in the dataset, ASV_00001, was identical to the V5-V7 region of a metagenome-assembled genome (MAG) reconstructed from the Baltic Proper (BACL30) and has been identified as dominant in the Baltic Sea [16,58]. Phylogenetic classification based on amino-acid classification included BACL30 in the S5.2 clade [16]; however this classification may have been biased by the lack of genome sequenced estuarine and freshwater SYN strains. In this study, ASV_00001 had 99% identity with the strain MW73D5, a freshwater strain included in clade A/B [12]. Most of the ASVs of the picocyanobacterial community in the Baltic Sea were more similar to freshwater strains rather than estuarine and marine strains, which suggest a freswater origin as opposed to a global brackish microbiome [58]. ASV_00001 showed high contributions during the summer, particularly at the LMO (up to 78%), in line with observations in other offshore locations [15,16]. However, the highest contributions took place in the cold months, indicating that BACL30 is well adapted to low temperature conditions.

This study provides a detailed description of picocyanobacterial seasonal abundance, biomass contribution and community composition during three years at a coastal and an offshore station in the Baltic Sea Proper, showing that SYN are highly adaptable and diverse. The results bridges the gap between phylogenetic classification and ecology. In a climate change scenario, longer and warmer summers could result in earlier picocyanobacterial blooms in the coast as a consequence of achieving optimal temperatures for S5.2 ecotypes earlier in the spring/summer season. This effect could be further magnified by earlier and more extensive blooms of N_2-fixing cyanobacteria resulting in higher NH_4 availability, that are projected as a consequence of global warming [76,77]. However, at offhore locations in the Baltic Proper, the picocyanobacterial summer bloom could be delayed since optimal temperature for clade A/B would take place later in the year. The results in this study highlight that besides temperature, water column stratification and nutrient availability also play an important role in picocyanobacterial dynamics and community composition.

Methods

Field Sampling

Sampling was carried out bi-weekly at the Linnaeus Microbial Observatory (LMO), an offshore station located 10 Km off the east coast of Öland (Sweden) and weekly at the K-station, a coastal station located in the city of Kalmar, Sweden during 2018–2020. The temperature and salinity were measured using a conductivity/temperature/depth sensor CTD® Castaway at the K-station and a CTD probe (AAQ 1186-H, Alec Electronics, Japan) at the LMO. To remove large particles, samples were filtered through a 200 µm mesh.

Nutrients and Chl a

Water for measuring dissolved inorganic nutrients (NH_4, NO_2 + NO_3 (hereafter referred to as NO_3), PO_4 and SiO_4,) was sampled and frozen at -20°C until analysis using standard protocols (UV-Spectrophotometer, [78]). For measuring Chl *a*, 50–200 mL seawater was filtered through duplicate 25 mm A/E glass fiber filters (~1 µm pore size, Pall life Sciences, Ann Arbor, MI, USA). Filters were incubated overnight in darkness in 5mL of ethanol (96%) and fluorescence was measured the following day using a fluorometer (Turner design Model #040, Tucson, USA) following the Jespersen & Christoffersen [79] protocol.

Phytoplankton abundance and community composition

Samples for phytoplankton identification (> 5µm diameter) were fixed in acid lugol (1% final concentration) and counted according to the Utermöhl method[80] using an inverted microscope (Nikon TMS, Tokyo, Japan). The phytoplankton carbon biomass concentration (mg C mL^{-1}) was derived from the cell abundance and carbon biomass [80,81]. In addition to the traditional taxonomy the genus *Aphanizomenon*, *Nodularia* and *Dolichospermum* were included in the group defined as N_2-fixers.

Picophytoplankton abundance

Samples to determine picophytoplankton abundance were fixed with glutaraldehyde solution Grade I 25% in H_2O (Sigma-Aldrich, Missouri, USA; 1% final concentration) and stored at -80°C until analysis. K-station samples until 12th May 2020 and LMO samples until 10th July 2019 were analyzed using a Cyflow® Cube8 flow cytometer (Partec®, Germany) at 10 µL s^{-1} while after that date a BD FACSverse (BD Biosciences) was used instead. Picophytoplankton were counted as three populations photosynthetic picoeukaryotes (PPE), phycoerythrin rich (PE-rich) SYN cells and phycocyanin rich (PC-rich) SYN based on the gating described in Alegria Zufia et al. [53]. The observations for PPE abundance variation are represented in Supplementary Figure S1. Gating and visualization of the flow cytometric data were carried out using FCSalyzer ver. 0.9.22-alpha [82] .

DNA extraction, PCR amplification and sequencing

Samples for DNA analysis were collected by filtering 400 mL of water through a 0.2µm Supor®-200 filter (Pall Corporation, USA). The filters were stored at -80°C until extraction. DNA was extracted using the FastDNA™ SPIN Kit for Soil from MP Biomedicals Inc according to manufacturer´s instructions with the addition of an incubation with proteinase-K (0.02 µg/µL, final concentration) at 55°C for one hour. Sample concentration was measured using an Invitrogen Qubit 2.0 fluorometer (Thermo Fisher Scientific Inc.). Sample purity was assessed using a Thermo Scientific™ NanoDrop 2000 spectrophotometer (Thermo Fisher Scientific Inc.). The V5-V7 hypervariable region of the 16 rDNA gene was amplified using the primers Cya-771F (5'-AGGGGAGCGAAAGGGATTA-3') and Cya-1294R (5'-GCCTACGATCTGAACTGAGC-3') described in [60]. The PCR reaction was prepared in duplicates for each sample using the Thermo Scientific Phusion High-Fidelity PCR Master Mix according to the manufacturer's instructions with a reaction volume of 25 µL. The PCR was performed on a T100™ Thermal Cycler (BIO RAD, USA) with an initial denaturation at 98°C for 30 seconds; 20 cycles of denaturation at 98°C for 10 seconds, annealing at 55°C for 1 minute and extension at 72°C for 5 seconds; and a final extension step at 72°C for 2 minutes. Amplicon sequences were purified with AMPure XP (Beckman Coulter, USA) according to manufacturer's instructions prior to performing the index PCR. Indexes were attached to individual samples using NEXTERA Dual indexes (Illumina Inc.) in a PCR with an initial denaturation at 98°C for 30 seconds; 12 cycles of denaturation at 98°C for 10 seconds, annealing at 62°C for 30 seconds and extension at 72°C for 5 seconds; and a final extension step at 72°C for 2 minutes. Amplicon sequences were purified again after index PCR with AMPure XP (Beckman Coulter, USA). The purified amplicons were quantified with Invitrogen Qubit 2.0 fluorometer (Thermo Fisher Scientific Inc.) and pooled at equimolar concentrations. Indexed samples were sequenced with Illumina MiSeq (Illumina Inc, USA) with 300 cycle paired-end sequencing.

Bioinformatics processing

The resulting reads were denoised and screened for chimera removal with ampliseq (v1.1, https://github.com/nf-core/ampliseq) which runs on QIIME2 (2019.10) [83] and DADA2 (1.10.0) [84] and

taxonomy assignment of the resulting amplicon sequencing variants (ASVs) were done using the SILVA 132 database with a 90% identity threshold. Among all sequences in the libraries, 95% belonged to cyanobacteria, of which 97% were classified as Synechococcales. Then, sequences were plotted in a phylogenetic tree to cross check that all of them indeed affiliated with Synechococcales; sequences that did not affiliate were excluded from further analyses. The number of sequences for each sample after each step of the quality control pipeline are specified in Supplementary Table S1.

Phylogenetic analysis

The ASVs that represented > 1% of the sequences in at least one sampling point were selected. To determine the phylogenetic clade affiliation, the closest representative sequences [60] were identified and retrieved using the BLASTn-Search engine in the NCBI database. Sequences were aligned using MAFFT v.7 [85] and a phylogenetic tree was constructed by the maximum likelihood method (ML) in MEGAX software [86] following the GTR + G + I model (bootstrap values inferred from 1000 replicates). Branches that did not associate with previously known clades were given new clade names. The resulting tree was edited using the interactive tree of Life (iTOL, http://itol.embl.de).

Statistical analysis

Datasets were rarefied to a sequence depth of 27819 sequences. All statistical analyses were performed using R version 3.6.1 [87] and the vegan package [88].

Partial least square regression

Partial least square regression (PLS) was used to evaluate the picocyanobacterial relationship with the following independent variables: *in situ* nutrients (NO_3 (µM), PO_4 (µM), SiO_2 (µM)), temperature (C°), salinity (PSU), stratification index (N^2; 10^{-3} s^{-2}), presence of N_2-fixers (mg C mL^{-1}) and total phytoplankton biomass (mg C mL^{-1}). The model was performed separately for PE-rich (cells mL^{-1}) and PC-rich (cells mL^{-1}) separately and by pooling together the data from K-station and LMO. All variables were $\log_{10}(x + 1)$ transformed for standardization. The stratification index was calculated following the Brunt-Väisälä frequency (3) [89]:

$$(3)\ N^2 = -\frac{g}{\rho}\frac{\rho_s - \rho_b}{H}$$

Where g is the gravitational acceleration (m s^{-2}), ρ is the average density of seawater (1.025 g cm^{-3}), ρ_s is the surface density (g cm^{-3}) and ρ_b is the density at the bottom (g cm^{-3}). The K-station is 3m deep, and thus all the water column is permanently in the photic zone. However, the calculated N^2 was ~ 0, indicating an unstable water column. Because of this, 1×10^{-3} s^{-2} values were assigned to all sampling dates in the K-station, indicating a strong stratification. The variable importance in projection (VIP) was used to determine the relative importance of the independent variables considered [90,91]. Variables were considered significant when VIP > 1.

Procrustes analysis

Procrustes analysis was used to compare correspondence analysis (CA) based on phylogenetic clades and ASVs. The goal of this analysis was to test whether the distribution of the phylogenetic clades was congruent with the distribution of ASVs. The significance of the association of the two datasets was later explored with a squared m12 test (999 permutations, P-value < 0.05).

Canonical correspondence analysis

A step-wise canonical correspondence analysis (CCA) (P-value = 0.05) was performed to identify the relationship of environmental and biotic variables to SYN community clade composition. The variables considered were: NO_3 (µM), PO_4 (µM), SiO_4 (µM), temperature (C°), salinity (PSU), stratification index (10^{-3} s^{-2}), phytoplankton biomass (mg C mL^{-1}), N_2-fixers biomass (mg C mL^{-1}), PE-rich (cells mL^{-1}) and PC-rich (cells mL^{-1}). To avoid type I errors, results were considered significant when P-value after Holm correction resulted in P-value < 0.05. All the independent variables were $\log_{10}(x + 1)$ transformed for standardization.

Declarations

Acknowledgements

We would like to thank Anders Månsson, Soran Mahmoudi, Maurice Hirwa, Christien Laber and Laura Bas Conn for assistance with the K-station sampling, Kalmar Kommun for access to Kallbadhuset where the K-station is located, Clara Pérez Martínez, Kristofer Bergström, Sabina Arnautovic, Camilla Karlsson, Emil Fridolfsson and Benjamin Pontiller for sampling at the LMO, EON, Northern Offshore Services (NOS), and the Provider crew for technical assistance during sampling at the LMO, Sonia Brugel from Umeå University for flow cytometry counts, Jasmine Weber-Pierson and Thi Quyen Nham for the nutrient analysis, Justyna Kobos and Lidia Nawrocka from University of Gdansk for the microscopic phytoplankton counts and Daniel Lundin and Emelie Nilsson for assistance on the genetic data analysis. Sequencing was performed by the SNP&SEQ Technology Platform in Uppsala. The facility is part of the National Genomics Infrastructure (NGI) Sweden and Science for Life Laboratory. The SNP&SEQ Platform is also supported by the Swedish Research Council and the Knut and Alice Wallenberg Foundation.

This work was supported by FORMAS (2017-00468) and Anna-Greta and Holger Crafoord Foundation (CR2019-0012) to HF and the Swedish governmental strong research program EcoChange.

Conflict of interest

None declared.

Data availability

The datasets generated and/or analysed during the current study are available in the NCBI repository, https://dataview.ncbi.nlm.nih.gov/object/PRJNA810944?reviewer=5biv7bdma5gho87ka1n2r6i8ov

References

1. Flombaum, P. *et al.* Present and future global distributions of the marine Cyanobacteria *Prochlorococcus* and *Synechococcus*. PNAS **110**, 9824–9829 (2013).
2. Honda, D. & Yokota, A. Detection of Seven Major Evolutionary Lineages in Cyanobacteria Based on the 165 rRNA Gene Sequence Analysis with New Sequences of Five Marine *Synechococcus* Strains. J Mol Evol **48**, 723–739 (1999).
3. Robertson, B. R., Tezuka, N. & Watanabe, M. M. Phylogenetic analyses of *Synechococcus* strains (cyanobacteria) using sequences of 16S rDNA and part of the phycocyanin operon reveal multiple evolutionary lines and reflect phycobilin content. Int. J. Syst. Evol. Microbiol. **51**, 861–871 (2001).
4. Stomp, M. *et al.* Adaptive divergence in pigment composition promotes phytoplankton biodiversity. Nature **432**, 104–107 (2004).
5. Albrecht, M., Pröschold, T. & Schumann, R. Identification of Cyanobacteria in a eutrophic coastal lagoon on the Southern Baltic Coast. Front. Microbiol. **8**, 1–16 (2017).
6. Bertos-Fortis, M. *et al.* Unscrambling cyanobacteria community dynamics related to environmental factors. Front. Microbiol. **7**, 625 (2016).
7. Guidi, L. *et al.* Plankton networks driving carbon export in the oligotrophic ocean. Nature **532**, 465–470 (2016).
8. Hunter-Cevera, K. R. *et al.* Seasons of Syn. Limnol. Oceanogr. **65**, 1–18 (2019).
9. Kuosa, H. Picoplanktonic algae in the northern Baltic Sea: seasonal dynamics and flagellate grazing. Mar. Ecol. Prog. Ser. **73**, 269–276 (1991).
10. Sathicq, M. B., Unrein, F. & Gómez, N. Recurrent pattern of picophytoplankton dynamics in estuaries around the world: The case of Río de la Plata. Mar. Environ. Res. **161**, 105136 (2020).
11. K.M., R. & Mitbavkar, S. Factors controlling the temporal and spatial variations in *Synechococcus* abundance in a monsoonal estuary. Mar. Environ. Res. **92**, 133–143 (2013).
12. Crosbie, N. D., Pöckl, M. & Weisse, T. Dispersal and phylogenetic diversity of nonmarine picocyanobacteria, inferred from 16S rRNA gene and cpcBA-intergenic spacer sequence analyses. Appl. Environ. Microbiol. **69**, 5716–5721 (2003).
13. Ernst, A., Becker, S., Wollenzien, U. I. A. & Postius, C. Ecosystem-dependent adaptive radiations ofpicocyanobacteria inferred from 16S rRNA and ITS-1 sequence analysis. Microbiology **149**, 217–228 (2003).
14. Sánchez-Baracaldo, P., Handley, B. A. & Hayest, P. K. Picocyanobacterial community structure of freshwater lakes and the Baltic Sea revealed by phylogenetic analyses and clade-specific quantitative PCR. Microbiology **154**, 3347–3357 (2008).

15. Hu, Y. O. O., Karlson, B., Charvet, S. & Andersson, A. F. Diversity of pico- to mesoplankton along the 2000 km salinity gradient of the baltic sea. Front. Microbiol. **7**, 679 (2016).
16. Larsson, J. *et al.* Picocyanobacteria containing a novel pigment gene cluster dominate the brackish water Baltic Sea. ISME J. **8**, 1892–1903 (2014).
17. Celepli, N. *et al.* Meta-omic analyses of Baltic Sea cyanobacteria: diversity, community structure and salt acclimation. Environ. Microbiol. **19**, 673–686 (2017).
18. Sánchez-Baracaldo, P., Handley, B. A. & Hayest, P. K. Picocyanobacterial community structure of freshwater lakes and the Baltic Sea revealed by phylogenetic analyses and clade-specific quantitative PCR. Microbiology **154**, 3347–3357 (2008).
19. Flombaum, P., Wang, W. L., Primeau, F. W. & Martiny, A. C. Global picophytoplankton niche partitioning predicts overall positive response to ocean warming. Nat. Geosci. **13**, 116–120 (2020).
20. Bopp, L. *et al.* Multiple stressors of ocean ecosystems in the 21st century: Projections with CMIP5 models. Biogeosciences **10**, 6225–6245 (2013).
21. Cabré, A., Marinov, I. & Leung, S. Consistent global responses of marine ecosystems to future climate change across the IPCC AR5 earth system models. Clim. Dyn. **45**, 1253–1280 (2015).
22. Wang, T., Chen, X., Qin, S. & Li, J. Phylogenetic and phenogenetic diversity of *Synechococcus* along a yellow sea section reveal its environmental dependent distribution and co-occurrence microbial pattern. J. Mar. Sci. Eng. **9**, 1018 (2021).
23. Tai, V. & Palenik, B. Temporal variation of *Synechococcus* clades at a coastal Pacific Ocean monitoring site. ISME J. **3**, 903–915 (2009).
24. Ahlgren, N. A. & Rocap, G. Diversity and distribution of marine *Synechococcus*: Multiple gene phylogenies for consensus classification and development of qPCR assays for sensitive measurement of clades in the ocean. Front. Microbiol. **3**, 1–24 (2012).
25. Rajaneesh, K. M., Mitbavkar, S., Anil, A. C. & Sawant, S. S. *Synechococcus* as an indicator of trophic status in the Cochin backwaters, west coast of India. Ecol. Indic. **55**, 118–130 (2015).
26. Campbell, L. & Carpenter, E. J. Characterization of phycoerythrin-containing *Synechococcus* spp. populations by immunofluorescence. J. Plankton Res. **9**, 1167–1181 (1987).
27. Stomp, M. *et al.* Colourful coexistence of red and green picocyanobacteria in lakes and seas. Ecol. Lett. **10**, 290–298 (2007).
28. Callieri, C. & Stockner, J. G. Freshwater autotrophic picoplankton: A review. J. Limnol. **61**, 1–14 (2002).
29. Liu, H., Jing, H., Wong, T. H. C. & Chen, B. Co-occurrence of phycocyanin- and phycoerythrin-rich *Synechococcus* in subtropical estuarine and coastal waters of Hong Kong. Environ. Microbiol. Rep. **6**, 90–99 (2014).
30. Haverkamp, T. *et al.* Diversity and phylogeny of Baltic Sea picocyanobacteria inferred from their ITS and phycobiliprotein operons. Environ. Microbiol. **10**, 174–188 (2008).

31. Rajaneesh, K. M. & Mitbavkar, S. Factors controlling the temporal and spatial variations in *Synechococcus* abundance in a monsoonal estuary. Mar. Environ. Res. **92**, 133–143 (2013).
32. Otero-Ferrer, J. L. *et al.* Factors controlling the community structure of picoplankton in contrasting marine environments. Biogeosciences **15**, 6199–6220 (2018).
33. Ploug, H. *et al.* Carbon, nitrogen and O_2 fluxes associated with the cyanobacterium Nodularia spumigena in the Baltic Sea. ISME J. **5**, 1549–1558 (2011).
34. Ohlendieck, U., Stuhr, A. & Siegmund, H. Nitrogen fixation by diazotrophic cyanobacteria in the Baltic Sea and transfer of the newly fixed nitrogen to picoplankton organisms. J. Mar. Syst. **25**, 213–219 (2000).
35. Klawonn, I. *et al.* Untangling hidden nutrient dynamics: rapid ammonium cycling and single-cell ammonium assimilation in marine plankton communities. ISME J. **13**, 1960–1974 (2019).
36. Kuo, J. *et al.* Picoplankton dynamics and picoeukaryote diversity in a hyper-eutrophic subtropical lagoon. J. Environ. Sci. Heal. **4**, 521–523 (2014).
37. Grébert, T. *et al.* Light color acclimation is a key process in the global ocean distribution of *Synechococcus* cyanobacteria. PNAS. **115**, E2010–E2019 (2018).
38. Urbach, E., Scanlan, D., Distel, D., Waterbury, J. & Chisholm, S. Rapid diversification of marine picophytoplankton with dissimilar light-harvesting structures inferred from sequences of *Prochlorococcus* and *Synechococcus* (cyanobacteria). *J. Mol. Biol.* **46**, 188–201 (1998).
39. Farrant, G. K. *et al.* Delineating ecologically significant taxonomic units from global patterns of marine picocyanobacteria. PNAS. **113**, E3365–E3374 (2016).
40. Rocap, G., Distel, D. L., Waterbury, J. B. & Chisholm, S. W. Resolution of *Prochlorococcus* and *Synechococcus* ecotypes by using 16S-23S ribosomal DNA internal transcribed spacer sequences. Appl. Environ. Microbiol. **68**, 1180–1191 (2002).
41. Mazard, S., Ostrowski, M., Partensky, F. & Scanlan, D. J. Multi-locus sequence analysis, taxonomic resolution and biogeography of marine *Synechococcus*. Environ. Microbiol. **14**, 372–386 (2012).
42. Huang, S. *et al.* Novel lineages of *Prochlorococcus* and *Synechococcus* in the global oceans. ISME J. **6**, 285–297 (2011).
43. Choi, D. H. & Noh, J. H. Phylogenetic diversity of *Synechococcus* strains isolated from the East China Sea and the East Sea. FEMS Microbiol. Ecol. **69**, 439–448 (2009).
44. Lee, M. D. *et al.* Marine *Synechococcus* isolates representing globally abundant genomic lineages demonstrate a unique evolutionary path of genome reduction without a decrease in GC content. Environ. Microbiol. **21**, 1677–1686 (2019).
45. Paerl, H. W. & Huisman, J. Climate: Blooms like it hot. Science. **320**, 57–58 (2008).
46. Fuller, N. *et al.* Clade-specific 16S ribosomal DNA oligonucleotides reveal the predominance of a single marine *Synechococcus* clade throughout a stratified water column in the Red sea. Appl. Environ. Microbiol. **69**, 2430–2443 (2003).

47. Scanlan, D. J. *et al.* Ecological genomics of marine Picocyanobacteria. Microbiol Mol Biol Rev. **73**, 249–299 (2009).
48. Mazard, S., Wilson, W. H. & Scanlan, D. J. Dissecting the physiological response to phosphorus stress in marine *Synechococcus* isolates (cyanophyceae). J. Phycol. **48**, 94–105 (2012).
49. Li, J. *et al. Synechococcus* bloom in the Pearl River Estuary and adjacent coastal area –With special focus on flooding during wet seasons. Sci. Total Environ. **692**, 769–783 (2019).
50. Zwirglmaier, K. *et al.* Global phylogeography of marine *Synechococcus* and *Prochlorococcus* reveals a distinct partitioning of lineages among oceanic biomes. Environ. Microbiol. **10**, 147–161 (2008).
51. Sohm, J. A. *et al.* Co-occurring *Synechococcus* ecotypes occupy four major oceanic regimes defined by temperature, macronutrients and iron. ISME J. **10**, 333–345 (2016).
52. Bunse, C. *et al.* High frequency multi-year variability in baltic sea microbial plankton stocks and activities. Front. Microbiol. **10**, 1–18 (2019).
53. Alegria Zufia, J., Farnelid, H. & Legrand, C. Seasonality of Coastal Picophytoplankton Growth, Nutrient Limitation and Biomass Contribution. Front. Microbiol. **12**, 1–13 (2021).
54. Granéli, E., Wallström, K., Larsson, U., Granéli, W. & Elmgren, R. Nutrient limitation of primary production in the Baltic Sea Area. Ambio. **19**, 142–151 (1990).
55. Mazur-Marzec, H. *et al.* Occurrence of cyanobacteria and cyanotoxin in the Southern Baltic Proper. Filamentous cyanobacteria versus single-celled picocyanobacteria. Hydrobiologia **701**, 235–252 (2013).
56. Stal, L. *et al.* BASIC: Baltic Sea cyanobacteria. An investigation of the structure and dynamics of water blooms of cyanobacteria in the Baltic Sea - Responses to a changing environment. Cont. Shelf Res. **23**, 1695–1714 (2003).
57. Herlemann, D. P. *et al.* Transitions in bacterial communities along the 2000 km salinity gradient of the Baltic Sea. ISME J. **5**, 1571–1579 (2011).
58. Hugerth, L. W. *et al.* Metagenome-assembled genomes uncover a global brackish microbiome. Genome Biol. **16**, 1–18 (2015).
59. Walve, J. & Larsson, U. Seasonal changes in Baltic Sea seston stoichiometry: The influence of diazotrophic cyanobacteria. Mar. Ecol. Prog. Ser. **407**, 13–25 (2010).
60. Huber, P. *et al.* Primer Design for an Accurate View of Picocyanobacterial Community Structure by Using High-Throughput Sequencing. Appl Environ Microbiol. **85**, 1–17 (2019).
61. Collos, Y. *et al.* Oligotrophication and emergence of picocyanobacteria and a toxic dinoflagellate in Thau lagoon, southern France. J. Sea Res. **61**, 68–75 (2009).
62. Bec, B., Husseini-Ratrema, J., Collos, Y., Souchu, P. & Vaquer, A. Phytoplankton seasonal dynamics in a Mediterranean coastal lagoon: Emphasis on the picoeukaryote community. J. Plankton Res. **27**, 881–894 (2005).
63. Hunter-Cevera, K. R. *et al.* Physiological and ecological drivers of early spring blooms of coastal phytoplankter. Science. **354**, 326–329 (2016).

64. Albertano, P., Di Somma, D. & Capucci, E. Cyanobacterial picoplankton from the central Baltic Sea: cell size classification by image analyzed fluorescence microscopy. J. Plankton Res. **19**, 1405–1416 (1997).
65. Paulsen, M. L. *et al. Synechococcus* in the Atlantic Gateway to the Arctic Ocean. Front. Mar. Sci. **3**, (2016).
66. Grinienė, E., Šulčius, S. & Kuosa, H. Size-selective microzooplankton grazing on the phytoplankton in the Curonian Lagoon (SE Baltic Sea). Oceanologia **58**, 292–301 (2016).
67. Tsai, A. Y., Gong, G. C., Huang, Y. W. & Chao, C. F. Estimates of bacterioplankton and *Synechococcus* spp. mortality from nanoflagellate grazing and viral lysis in the subtropical Danshui River estuary. Estuar. Coast. Shelf Sci. **153**, 54–61 (2015).
68. Camacho, A., Miracle, M. R. & Vicente, E. Which factors determine the abundance and distribution of picocyanobacteria in inland waters? A comparison among different types of lakes and ponds. Arch. fur Hydrobiol. **157**, 321–338 (2003).
69. Berry, D. L. *et al.* Shifts in Cyanobacterial Strain Dominance during the Onset of Harmful Algal Blooms in Florida Bay, USA. Microb. Ecol. **70**, 361–371 (2015).
70. Zborowsky, S. & Lindell, D. Resistance in marine cyanobacteria differs against specialist and generalist cyanophages. PNAS. **116**, 16899–16908 (2019).
71. Wall, C. C., Rodgers, B. S., Gobler, C. J. & Peterson, B. J. Responses of loggerhead sponges Spechiospongia vesparium during harmful cyanobacterial blooms in a sub-tropical lagoon. Mar. Ecol. Prog. Ser. **451**, 31–43 (2012).
72. Glibert, P. M. *et al.* Pluses and minuses of ammonium and nitrate uptake and assimilation by phytoplankton and implications for productivity and community composition, with emphasis on nitrogen-enriched conditions. Limnol. Oceanogr. **61**, 165–197 (2016).
73. Herbert, R. A. Nitrogen cycling in coastal marine ecosystems. FEMS Microbiol. Rev. **23**, 563–590 (1999).
74. Cai, J., Hodoki, Y. & Nakano, S. ichi. Phylogenetic diversity of the picocyanobacterial community from a novel winter bloom in Lake Biwa. Limnology **22**, 161–167 (2021).
75. Guyet, U. *et al.* Synergic effects of temperature and irradiance on the physiology of the marine *Synechococcus* strain WH7803. Front Microbiol **11**, 1707 (2020).
76. Neumann, T. *et al.* Extremes of temperature, oxygen and blooms in the baltic sea in a changing climate. Ambio **41**, 574–585 (2012).
77. Andersson, A. *et al.* Projected future climate change and Baltic Sea ecosystem management. Ambio **44**, 345–356 (2015).
78. Valderrama, J. C. Methods of nutrient analysis. in *Manual on Harmful Marine Microalgae* (eds. Hallagraeff, G. M., Anderson, D. M. & Cembella, A. D.) 251–268 (IOC Manuals and Guides, 1995).
79. Jespersen, A. M. & Christoffersen, K. Measurements of chlorophyll-a from phytoplankton using ethanol as extraction solvent. Arch. für Hydrobiol. **109**, 445–454 (1987).

80. Edler, L. *Recommendations on methods for marine biological studies in the Baltic Sea. Phytoplankton and chlorophyll*. (Baltic Marine Biologists BMB (Sweden), 1979).
81. HELCOM Phytoplankton Expert Group. Phytoplankton biovolume and carbon content. https://www.ices.dk/data/Documents/ENV/PEG_BVOL.zip, (2013).
82. Mostböck, S. FCSalyzer. https://sourceforge.net/projects/fcsalyzer (2021).
83. Gregory Caporaso, J. *et al.* QIIME allows analysis of high-throughput community sequencing data. (2010).
84. Callahan, B. *et al.* DADA2: High-resolution sample inference from Illumina amplicon data. **13**, 581–583 (2016).
85. Katoh, K., Misawa, K., Kuma, K. I. & Miyata, T. MAFFT: A novel method for rapid multiple sequence alignment based on fast Fourier transform. Nucleic Acids Res. **30**, 3059–3066 (2002).
86. Kumar, S., Stecher, G., Li, M., Knyaz, C. & Tamura, K. MEGA X: Molecular evolutionary genetics analysis across computing platforms. Mol. Biol. Evol. **35**, 1547–1549 (2018).
87. R Core Team. R: A Language and Environment for Statistical Computing. R Foundation for Statistical Computing, Vienna, Austria. R version 3.5.1. https://www.R-proje ct.org/. (2019).
88. Oksanen, J. *et al.* Package 'vegan'. (2020).
89. Gill, A. E. Atmosphere-ocean Dynamics. (1982). *Academic press.*
90. Li, X., Wang, Y., Li, J. & Lei, B. Physical and socioeconomic driving forces of land-use and land-cover changes: A Case Study of Wuhan City, China. *Discret. Dyn. Nat. Soc.* 2016, (2016).
91. Paliy, O. & Shankar, V. Application of multivariate statistical techniques in microbial ecology. Mol. Ecol. **25**, 1032–1057 (2016).

Figures

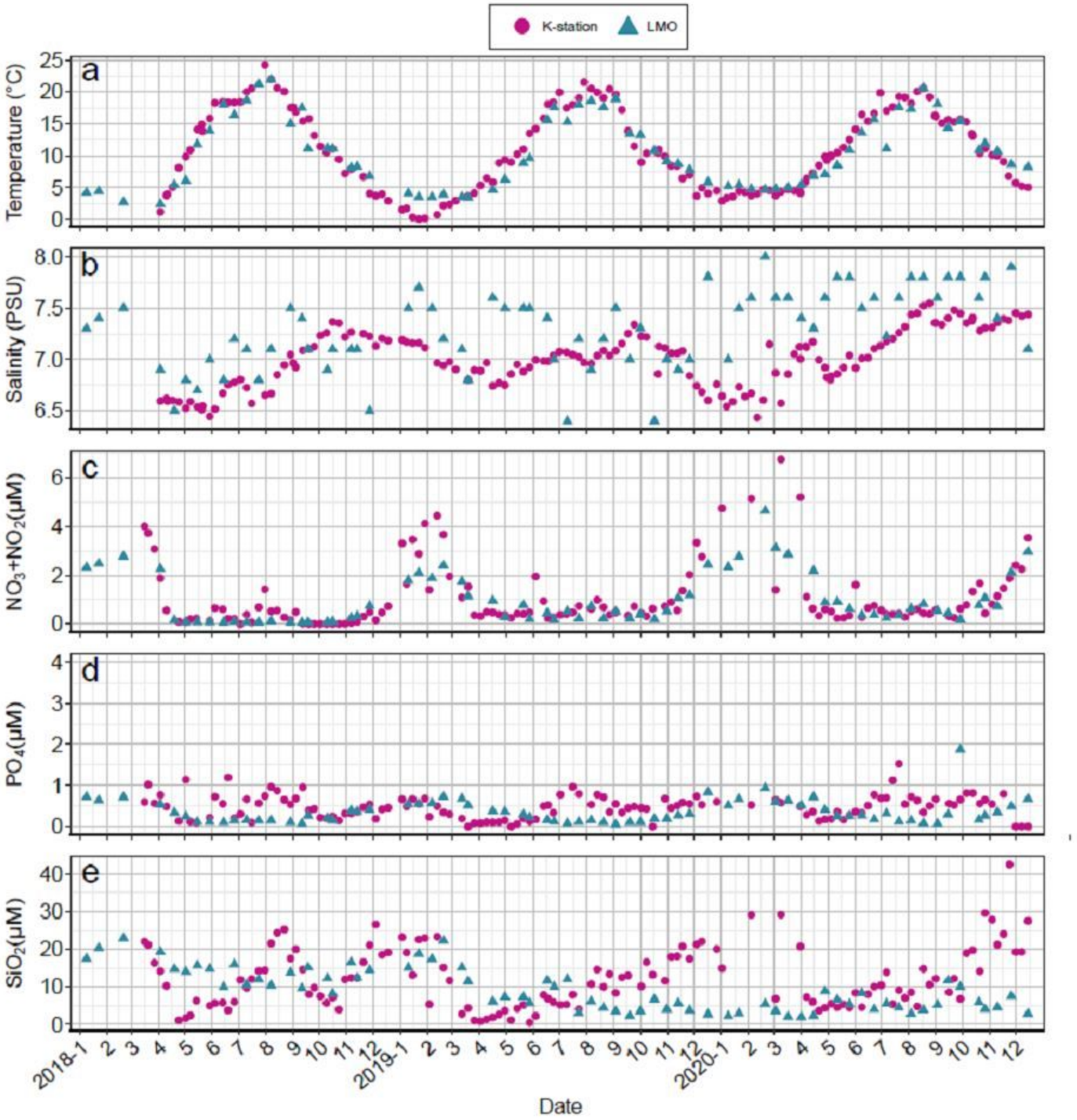

Figure 1

K-station circles and LMO (triangles) measurements for (A) temperature (°C), (B) salinity, (C) NO_3 (μM), (D) PO_4 (μM) and (E) SiO_4

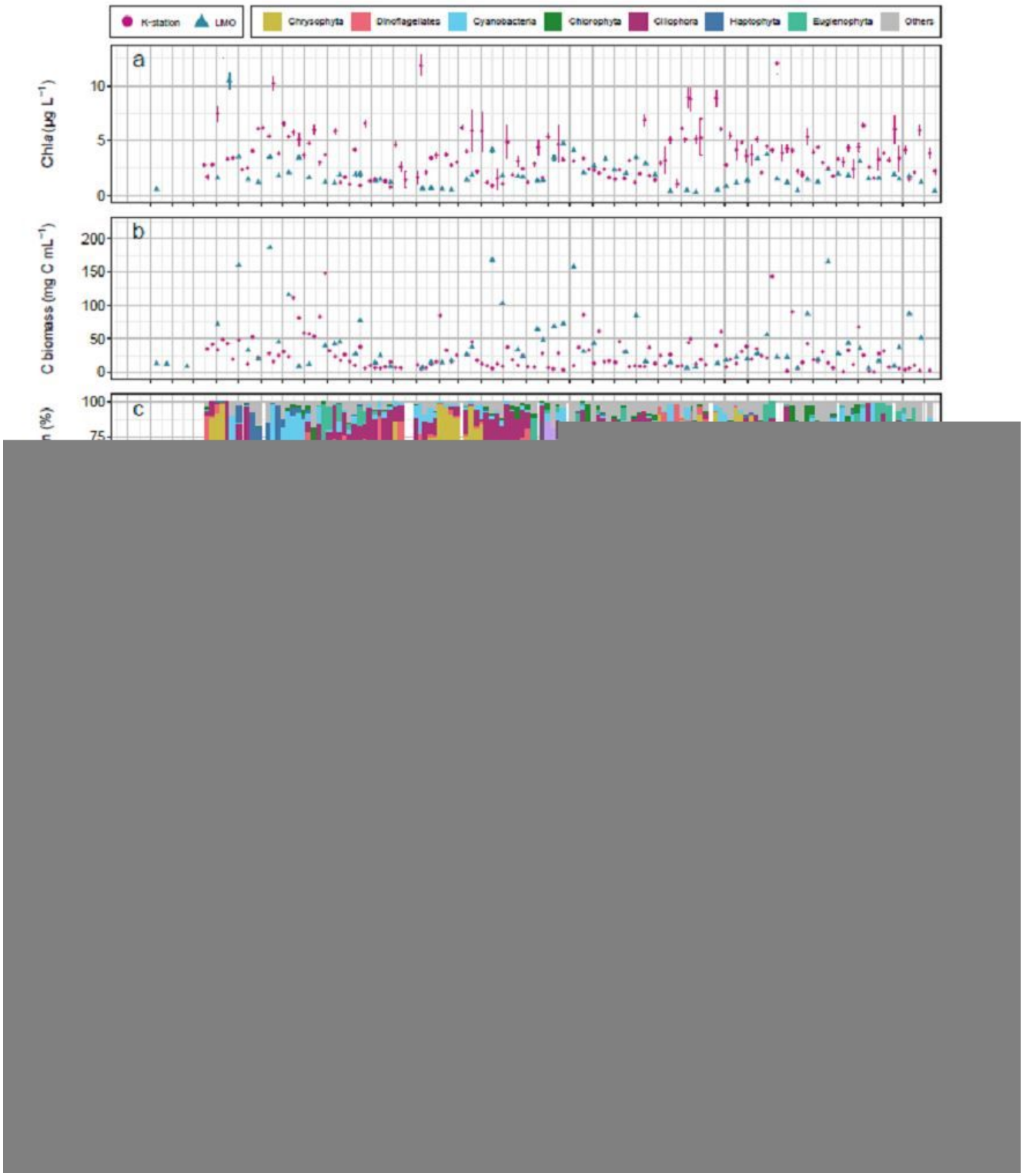

Figure 2

K-station and LMO measurements for (A) Chl a (μg L^{-1}), (B) total phytoplankton (>5 μm in diameter) carbon biomass concentration (mg C mL^{-1}) based on microscopy, (C and D) relative contribution of phytoplankton divisions (>5 μm in diameter) based on microscopy, (E) PE-rich (cells mL^{-1}) and (F) PC-rich (cells mL^{-1}).

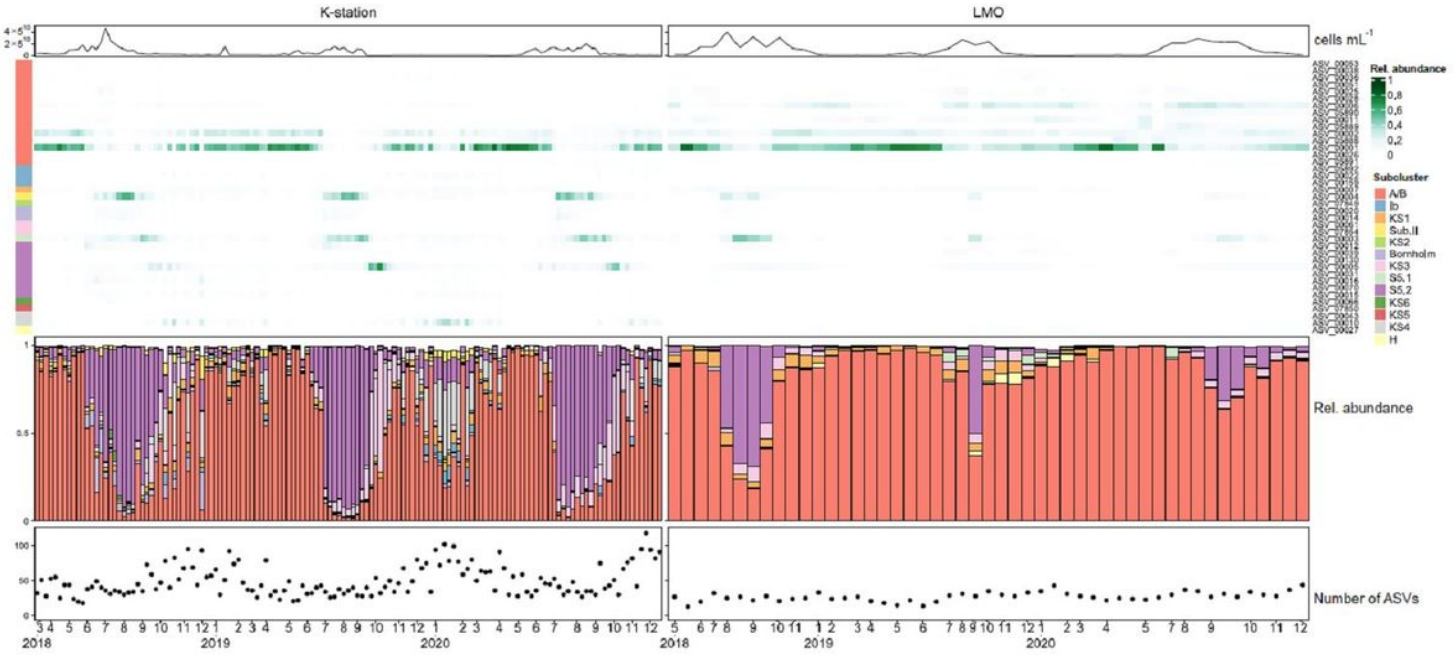

Figure 3

Relative abundance of all the ASVs with contribution higher than 1% to the total Synechococcus community in the K-station and LMO. The line plot on top represents total picocyanobacterial abundance for each sampling point. The heatmap represents the relative contribution of each ASV on each sampling point. The color code on the left indicates the clade of each ASV represented on the heatmap. The bottom barplot indicates the relative contribution of each subgroup/clade to the total Synechococcus community. The bottom dot plot indicates the species richness on each sampling point.

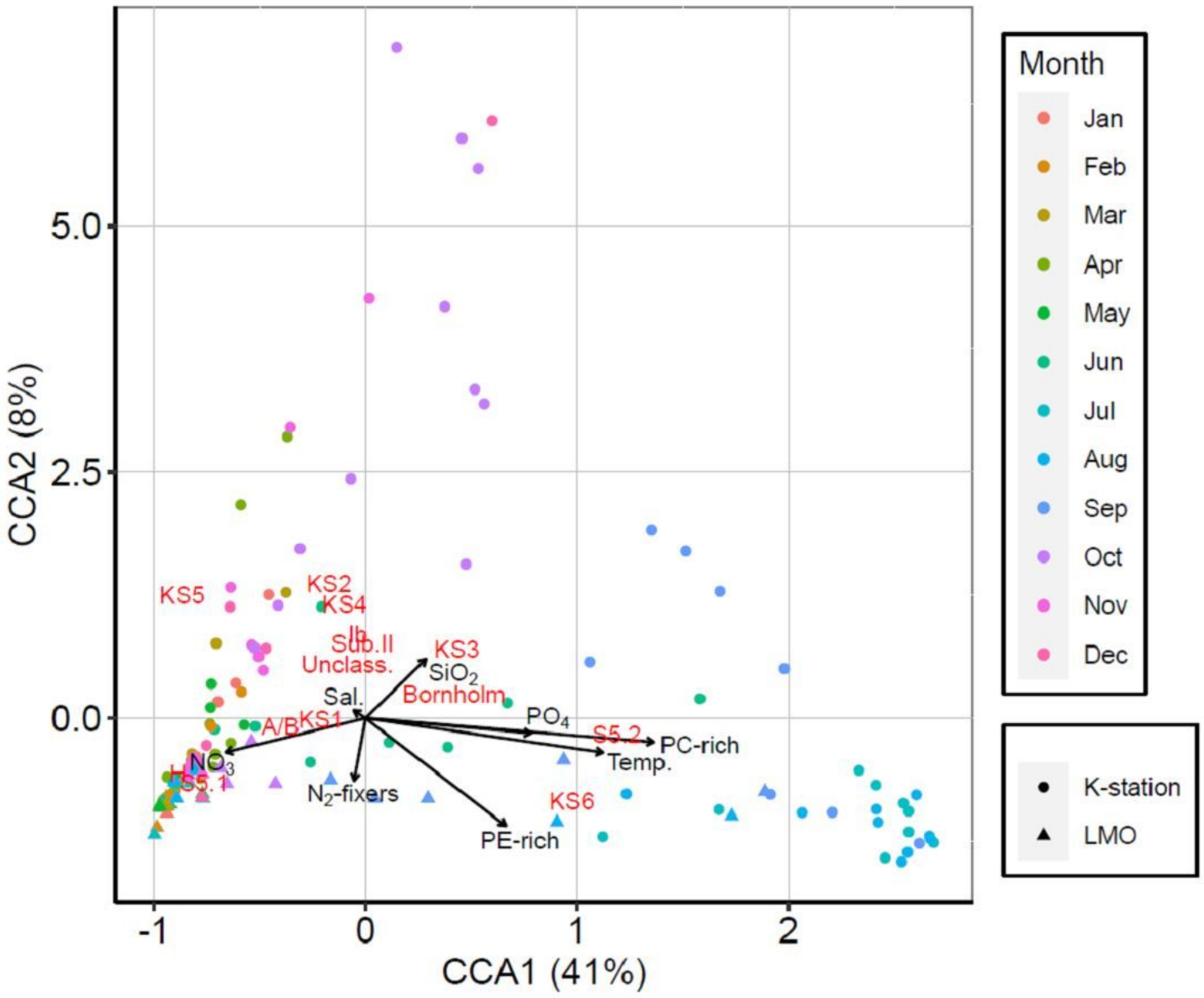

Figure 4

CCA analysis showing the relationships between environmental variables and picocyanobacterial community composition. Only variables that are significant are shown.

Supplementary Files

This is a list of supplementary files associated with this preprint. Click to download.

- manIIsuppsubmission1.pdf